Rapid response of Helheim Glacier, Greenland, to climate variability over the last century

Camilla S. Andresen[1*], Fiammetta Straneo[2], Mads Hvid Ribergaard[3], Anders A. Bjørk[4], Thorbjørn J. Andersen[5], Antoon Kuijpers[1], Niels Nørgaard-Pedersen[1], Kurt H. Kjær[4], Frands Schjøth[6], Kaarina Weckström[1], Andreas P. Ahlstrøm[1]

[1]*Geological Survey of Denmark and Greenland, Department of Marine Geology and Glaciology, Øster Voldgade 10, 1350 Copenhagen K, Denmark*

[2]*Department of Physical Oceanography, Woods Hole Oceanographic Institution, Woods Hole, Massachusetts 02543, USA*

[3]*Danish Meterological Institute, Centre for Ocean and Ice, Lyngbyvej 100, 2100 Copenhagen Ø, Denmark*

[4]*Centre for GeoGenetics, Natural History Museum, Øster Voldgade 5-7, 1350 Copenhagen K, Denmark*

[5]*Institute for Geology and Geography, Øster Voldgade 10, Univ. of Copenhagen, 1350 Copenhagen K, Denmark*

[6]*Geological Survey of Denmark and Greenland, Geological Data Centre, Øster Voldgade 10, 1350 Copenhagen K, Denmark*

** email: csa@geus.dk*

During the early 2000s the Greenland Ice Sheet experienced the largest ice mass loss observed on the instrumental record[1], largely as a result of the acceleration, thinning and retreat of major outlet glaciers in West and Southeast Greenland[2-5]. The quasi-simultaneous change in

the glaciers suggests a common climate forcing and increasing air[6] and ocean[7-8] temperatures have been indicated as potential triggers. Here, we present a new record of calving activity of Helheim Glacier, East Greenland, extending back to c. 1890 AD. This record was obtained by analysing sedimentary deposits from Sermilik Fjord, where Helheim Glacier terminates, and uses the annual deposition of sand grains as a proxy for iceberg discharge. The 120 year long record reveals large fluctuations in calving rates, but that the present high rate was reproduced only in the 1930s. A comparison with climate indices indicates that high calving activity coincides with increased Atlantic Water and decreased Polar Water influence on the shelf, warm summers and a negative phase of the North Atlantic Oscillation. Our analysis provides evidence that Helheim Glacier responds to short-term (3-10 years) large-scale oceanic and atmospheric fluctuations.

The forcings behind the early 2000s rapid increase in mass loss from the Greenland Ice Sheet[1] are still debated. It is unclear if the mass loss will continue in the near future and, if so, at what rate. These uncertainties are a consequence of our limited understanding of mechanisms regulating ice sheet variability and the response of fast flowing outlet glaciers to climate variability. In southeast Greenland, Helheim Glacier, one of the regions largest glaciers thinned, accelerated and retreated during the period 2003-2005[4] and while it has since slowed down and re-advanced[9], it has still not returned to its pre-acceleration flow rates.

It has been suggested that warming[8,10] and/or inflow variability[11-12] of the nearby subsurface ocean currents triggered the acceleration, but to establish a causal relation between glacier and climate variability, long-term records are needed. Here we present three high-resolution (1-3 years pr sample) sedimentary records from Sermilik Fjord (Fig. 1 and Supplementary Information) that capture the 2001-2005 episode of mass loss, and use them to reconstruct the

calving variability of Helheim Glacier over the past 120 years. Next this record is compared with records of climate indices.

Helheim Glacier discharges in the deep (600-900 m) Sermilik Fjord, which is connected with two deep troughs (500-700 m) that transect the shallow shelf (100-200 m) allowing exchange with shelf waters. The fjord is characterized by an upper 100-150 m thick layer of Polar Water (PW) from the East Greenland Current (EGC) and a deeper layer (500 m thick) of warm (3.5-4°C) and saline Atlantic Water (AW) from the North Atlantic Current[11] with the latter primarily driving submarine melting[12]. At the northern end the fjord branches into three smaller fjords, each containing calving glaciers. Of these, Helheim Glacier, is one of the most prolific iceberg-exporters in Greenland[1] whereas the two northern glaciers, Midgaard and Fenris Glaciers, are smaller and far less discharging[13]. The fjord is mostly sea-ice covered from January to June and a large ice-mélange extends year-round in front of Helheim Glacier.

Three sediment cores were collected (Fig. 1) and age models for the last 120 years were established on the basis of ^{210}Pb geochronology (Supplementary Fig. S2). The massive diamicton facies in the cores is produced by delivery of heterogeneous debris from drifting icebergs, commonly referred to as ice rafted debris, IRD (clay, silt, sand and pebbles) and to the down-fjord diminishing input of fine mud (clay and silt) suspended in the turbid melt water plume extending from the base of Helheim Glacier. This lithofacies interpretation is in accordance with the findings from other East Greenland fjords with marine-terminating glaciers[14-15].

To reconstruct a record of calving activity of Helheim Glacier it is assumed that changes in IRD deposition rate are directly related to changes in calving activity through iceberg rafting. This is supported by a study from the nearby Kangerdlugssuaq Fjord showing that the mean annual calving rate dominates the IRD deposition rates, whereas the influence of temperature on melting of icebergs is far less important[16]. The sand fraction is used as a proxy for IRD since sand

grains are too large (63-1000 μm) to be carried in suspension by the melt water plume and thus allow differentiation between the plume and icebergs. Accordingly, we propose that increased sand deposition reflects increased iceberg calving from Helheim Glacier and to a far less extent also from Midgaard and Fenris Glacier (Supplementary Information).

Iceberg residence time in the mélange is less than a year (K. Scharrer, personal communication, 2011) implying that variations in IRD entrainment over time does not significantly affect the variability in sand deposition rates down-fjord over the investigated time span (Supplementary Information).

Sand deposition rates in the three cores vary both in magnitude and variability (Fig 2a-c). The mean rate decreases down-fjord, consistent with the notion that icebergs become progressively IRD depleted as they transit down-fjord[15,17]. Generally the multi-decadal variability is similar, but ER13, the closest to Helheim, shows higher-frequency variability than ER07 and ER11. This is attributed to the initial high particle fluxes in the melt water plume from Helheim Glacier decaying abruptly south of ER13[12]. This favours deposition of larger amounts of suspended mud at ER13 thus diluting the IRD sand fraction and allowing higher time resolution compared with ER07 and ER11 (Fig. S4). Differences in the timing of the high-frequency variability are attributed to factors such as wind, fjord circulation and sea-ice cover, which affect iceberg routing[16] and hence the local iceberg rafting. Thus, to obtain a mean sand deposition rate time series for Sermilik Fjord, we created a composite record by averaging the sand deposition rates of the three cores (Fig. 2d) under the assumption that the average of the three cores is indicative of the mean deposition rate within most of the fjord. The validity of the composite sand deposition record as a proxy for the calving history of Helheim Glacier is supported by its agreement with changes in its front position according to satellite data and historical aerial photographs (Fig 2d).

The reconstructed 120 year long calving record from Helheim Glacier shows calving maxima and minima lasting 2-5 years and often bundled into longer episodes of 5-10 years. Two pronounced calving maxima are observed: one during the last 10 years, the other in the late 1930s/early1940s. The long term calving increase is likely due to a shift from the Little Ice Age conditions, which were characterised by low air temperatures and strong PW influence in the Denmark Strait region and ended after 1900 AD here[18].

Most of the climate-related mechanisms proposed to explain glacier acceleration and increased calving invoke increased local air and/or ocean temperatures. Warming summer air temperatures will increase surface melt which, in turn, can affect the glacier by increasing sliding[19] (though this process is small for Helheim Glacier[20]), by destabilizing the glacier's tongue by feeding its crevasses[21], or enhance submarine melting if released at depth in the fjord[22]. Increased ocean temperatures will also enhance submarine melt rates and, by changing the characteristics at the terminus, influence glacier stability[7,23]. Both ocean and air warming can reduce sea-ice formation in the fjord and within the ice mélange in front of the glacier, potentially increasing the calving rate by destabilizing the glacier tongue[17].

Helheim Glacier's calving record is compared with local oceanic and atmospheric variability to determine if a statistically significant correlation exists between them (Fig 3). Ocean variability is influenced by both the surface PW and the subsurface AW. Since there are no long-term ocean measurements from Sermilik Fjord or the nearby shelf, we rely on the upstream/near-source variability of the two watermasses (Supplementary Information) and the finding that they are continuously renewed via exchange with the shelf[11]. For AW we use direct measurements of sea surface temperature from a region south of Iceland where AW extends to the surface (Fig. 3b). For PW variability, we use changes in the northernmost multiyear sea-ice extent off Southwest Greenland (Storis Index[24]) assuming that it is correlated with PW variability (Fig. 3c).

Hydrographic variability on the shelf mostly reflects changes in the relative volume of AW and PW, thus the AW and PW indices were combined into a Shelf Index (Fig. 3d & Supplementary Fig. S6) - a positive Shelf Index indicates a thicker and warmer AW (at the expense of PW) and vice versa. The Shelf Index is validated via independent data sources in the Supplementary Information. Air temperature variability is taken from the observed summer temperatures near Tasiilaq[25] (Fig. 3F). Finally, we examine the correlation between calving activity and the winter time North Atlantic Oscillation (NAO) Index[26], representative of the dominant mode of atmospheric climatic variability in the North Atlantic region (Fig. 3e).

Although non-climatic factors intrinsic to Helheim Glacier (e.g. glacier bed topography; internal glacier dynamics) are expected to influence calving activity[27], our analysis indicates that a significant fraction of the calving variability of Helheim Glacier since 1890 AD is consistent with increased AW (temperature and/or volume), decreased PW, a positive Shelf Index, increased summer air temperatures and a negative NAO Index as implied by significant correlations on the bulk data sets (Table 1 & Supplementary Information).

To investigate the timescales involved, we first consider the correlation between the 25 year low-pass filtered calving and climate records (Supplementary Fig. S7). This shows that on multi-decadal timescales, calving is mostly linked with synchronous changes in the source AW and the local summer air temperature, which, in turn, track the Atlantic Multi-decadal Oscillation (AMO[28]). Given the regional oceanic and atmospheric covariance on these timescales, it is not possible to separate their relative contribution to glacier variability.

On shorter term timescales (3-10 years) we find that the correlation of the residual calving variability and the residual climate variability is significant only for the NAO Index and the Shelf Index (Table 1). The high correlation with the NAO Index is expected since local winds and air temperatures as well as variability in both the PW and AW source regions often co-vary with the

NAO[29] on these timescales. A negative NAO phase, in particular, is associated with a warm subpolar gyre and increased penetration of AW on the shelf[8]. However, this analysis also indicates that episodes of increased PW inflow, e.g. the Great Salinity Anomalies (GSAs) between 1965 and 1972 and during the early 1980s and early 1990s[30] (Fig. 3c), were associated with diminished calving activity, likely due to stabilization of the glacier terminus and mélange and/or reduced AW penetration on the shelf.

The climate characteristics found for a composite of the ten highest short-term calving episodes (HC1-HC10 in Fig. 3a & Supplementary Table 1) support the conclusion that the Shelf Index and the phase of the NAO are significant players in modulating short-term calving variability.

Our analysis indicates that the recent increase in calving activity observed at Helheim Glacier is not unique but that a similarly large event occurred in the late 1930s/early 1940s (HC6 Fig. 3a). These two episodes occurred at times when the temperature of the AW source was high (positive/warm AMO phase) *and* the PW export was record low (even if fluctuating). The NAO Index was also frequently negative, though not markedly more than during many of the other calving episodes. Interestingly, both episodes are characterised by record high summer temperatures since 1895 (1939, 1941 and 2003). These conditions likely resulted in increased surface and submarine melt which may have contributed to the marked mass loss from Helheim Glacier.

Our study provides evidence that Helheim Glacier responds to changes in atmosphere-ocean variability on time-scales as short as a few years. Therefore the prediction of future ice sheet mass balance changes associated with dynamic adjustments from outlet glaciers needs to incorporate atmosphere-ocean climate models that are capable of reproducing the regional variability on these same timescales.

Methods summary

Core chronologies were established by measuring the ^{210}Pb and ^{137}Cs activity and mass accumulation rates were estimated. Grain size distribution was analysed by a Malvern Mastersizer 2000 laser particle sizer. The cumulative volume percentage was determined for the clay and silt fraction (<63 μm) and the sand fraction (63-1000 μm). X-ray radiography (Supplementary Fig. S1) and grain size analysis (Supplementary Fig. S3) of the cores reveals diamicton facies in all three cores with a mean content of sand of 9%, 22% and 18 %, in cores ER13, ER07 and ER11 respectively, reflecting a more condensed stratigraphy of the two latter cores. Sand deposition rates (iceberg rafting) were estimated as the flux of sand grains (g m^{-2} yr^{-1}) and the composite was produced as an average of the three cores. For documentation of past glacier margin positions, images from satellite and aerial photographs were geo-referenced using ortho-rectified aerial photographs from 1981 with a 2-meter spatial resolution. Time series of annual mean SST for an area south of Iceland (20−30°W, 60−63°N) were constructed using mainly the ICES database (www.ices.dk) and are used as a proxy for AW temperatures. A time series of maximal multiyear sea-ice extent along southwest Greenland in May, June and July was used as a proxy for the volume of PW. The Shelf Index was produced by normalizing these proxy records and further subtracting the resultant PW Index from the AW Index. The Pearson correlation coefficients between the calving record and climate indices were calculated by filtering the data with a 3 point running mean (except the calving record). All data were linearly detrended and a 25 year low pass Fourier filter was applied to differentiate between longer- and shorter-term variability. The residuals were estimated by subtracting the low-passed filtered data from the 3-year filtered and linearly detrended dataset. A detailed description of methods is given in the Supplementary Information.

References

1 Rignot, E. & Kanagaratnam, P. Changes in the velocity structure of the Greenland Ice Sheet. *Science* **311,** 986-990 (2006).

2. Joughin, I., Abdalati, W. & Fahnestock, M. Large fluctuations in speed on Greenland's Jakobshavn Isbræ glacier. *Nature* **432**, 608-610 (2004).

3. Luckman, A., Murray, T., de Lange, R., & Hanna, E. Rapid and synchronous ice-dynamic changes in East Greenland, *Geophys. Res. Lett.* **33**, L03503, doi:10.1029/2005GL025428 (2006).

4. Stearns, L. A. & Hamilton, G. S. Rapid volume loss from two East Greenland outlet glaciers quantified using repeat stereo satellite imagery. *Geophys. Res. Lett.* **34,** L05503, doi:10.1029/2006GL028982 (2007).

5. Howat, I. M., Joughin, I. & Scambos, T.A. Rapid changes in ice discharge from Greenland Outlet Glaciers. *Science* **315,** 1559-1561 (2007).

6. Box, J.E., Yang, L. Browmich, D.H & Bai, L-S. Greenland ice sheet surface air temperature variability: 1840-2007, *J. Climate* **22(14)**, 4029-4049, (2009).

7. Holland, D. M., Thomas, R. H., de Young, Ribergaard, M. H., and Lyberth, B. Acceleration of Jakobshavn Isbrae triggered by warm subsurface ocean waters, *Nature Geoscience* **1**, 659–664 (2008).

8. Murray, T., *et al.* Ocean regulation hypothesis for glacier dynamics in southeast Greenland and implications for ice sheet mass changes. *J. Geophys. Res.* **115**, F03026, doi:10.1029/2009JF001522 (2010).

9. Joughin, I. *et al.* Ice-front variation and tidewater behavior on Helheim and Kangerdlugssuaq Glaciers, Greenland. *J. Geophys. Res*. **113**, F01004, doi:10.1029/2007JF000837 (2008).

10. Nick, F. M., Vieli, A., Howat, I., M. & Joughin, I. Large-scale changes in Greenland outlet glacier dynamics triggered at the terminus. *Nature Geoscience* **2,** 110-114 (2009).

11. Straneo, F. *et al* . Rapid circulation of warm subtropical waters in a major glacial fjord in East Greenland. *Nature Geoscience* **3**, 182-186 (2010)

12. Straneo, F. *et al*. Impact of fjord dynamics and glacial runoff on the circulation near Helheim Glacier. *Nature Geoscience* **4**, 322–327, (2011).

13. Mernild, S. H. *et al.* Freshwater flux to Sermilik Fjord, SE Greenland. *The Cryosphere* **4**, 453–465 (2010).

14. Syvitski, J. P. M., Andrews, J. T., and Dowdeswell, J. A. Sediment deposition in an iceberg-dominated Glacimarine Environment, East Greenland: Basin Fill Implications. *Global and Planetary Change* **12**, 251-270 (1996).

15. Dowdeswell, J.A. *et al*. An origin for laminated glacimarine sediments through sea-ice build-up and suppressed iceberg rafting. Sedimentology 47, 557-576 (2000).

16. Mugford, R.I. & Dowdeswell, J. A. Modeling iceberg-rafted sedimentation in high-latitude fjord environments. *Journal of Geophysical Research* **115**, F03024, doi:10.1029/2009JF001564 (2010).

17. Amundson, J. M. et al. Ice mélange dynamics and implications for terminus stability, Jakobshavn Isbræ, Greenland, J. Geophys. Res., 115, F01005, doi:10.1029/2009JF001405 (2010).

18. Jennings, A.E. & Weiner, N.J. Environmental changes in eastern Greenland during the last 1300 years: evidence from foraminifera and lithofacies changes in Nansen Fjord, 68ºN. *The Holocene* **6 (2)**, 179–191 (1996).

19. Zwally, H. J. *et al.* Surface meltinduced acceleration of Greenland ice-sheet flow. *Science* **297**, 218–222 (2002).

20. Andersen, M. L., *et al.* Spatial and temporal melt variability at Helheim Glacier, East Greenland, and its effect on ice dynamics. J. Geophys. Res. **115**, F04041, doi:10.1029/2010JF001760 (2010).

21. Benn, D. I., Hulton, N. R. J. & Mottram R. H. "Calving laws","sliding laws" and the stability of tidewater glaciers. *Ann. Glaciol*. **46**, 123–130 (2007).

22. Motyka, R. J., M. Truffer, M. Fahnestock, J. Mortenson, S. Rysgaard, and I. Howat. Submarine Melting of the 1985 Jakobshavn Isbrae Floating Ice Tongue and the triggering of the current retreat. *J. Geophys. Res*., doi:10.1029/2009JF001632 (2011).

23. Thomas, R. H. *et al*. Substantial thinning of a major east Greenland outlet glacier. *Geophys. Res. Lett.* **27**, 1291–1294 (2000).

24. Schmith, T., & Hansen, C. Fram Strait Ice Export during the Nineteenth and Twentieth Centuries Reconstructed from a Multiyear Sea Ice Index from Southwestern Greenland. *Journal of Climate* **16**, 2782−2791 (2003).

25**.** Cappelen, J. (ed) DMI Daily Climate Data Collection 1873-2010, Denmark, The Faroe Islands and Greenland - including Air Pressure Observations 1874-2010 (WASA Data Sets). *DMI Technical Report* **11-06** (2011).

26. Hurrell, J. W. Decadal trends in the North Atlantic Oscillation: Regional temperatures and precipitation, Science, 269, 676– 679 (1995).

27. Warren, C. R. Iceberg calving and the glacioclimatic record. *Progress in Physical Geography*, **16**, 253-282 (1992).

28. Schlesinger, M. E., & Ramankutty, N. An oscillation in the global climate system of period 65-70 years. Nature 367, 723-726 (2004).

29. Dickson *et al*. The Arctic Ocean response to the North Atlantic Oscillation. *Journal of Climate* **13**, 2671-2696 (2000).

30. Belkin, I.M. Propagation of the "Great Salinity Anomaly" of the 1990s around the northern North Atlantic. *Geophysical Research Letters* **31**, L08306, doi:10.1029/2003GL019334 (2004).

Author contributions

APA, CSA and AKU conceived the study and CSA and NNP conducted fieldwork. CSA is main responsible for data interpretation, sediment core data analysis and led the writing of the paper. FSt contributed expertise on oceanography, statistical analysis and data interpretation and MHRI provided the oceanographic data compilation south of Iceland and updated the Storis Index from 2000 to 2008. AAB and KHK are responsible for glacier image analysis. TJA measured the ^{210}Pb and ^{137}Cs activities. FSc compiled bathymetry data into the map. All authors contributed to data interpretation and writing of the manuscript.

Request for material

Corresponding author: Camilla S. Andresen. The calving record and Shelf Index can be requested from Camilla S. Andresen (csa@geus.dk); AW proxy dataset can be requested from Mads Hvid Ribergaard (mhri@dmi.dk) and Storis Index can be requested from Mads Hvid Ribergaard or Torben Schmith (ts@dmi.dk).

Acknowledgements

This study has been supported by Geocenter Denmark in financial support to the SEDIMICE project. CSA was supported by the Danish Council for Independent Research | Nature and Universe (Grant no. 09-064954/FNU). FSt was supported by NSF ARC 0909373 and by WHOI's Ocean and Climate Change Institute and MHRI was supported by the Danish Agency for Science, Technology and Innovation. We thank Y.O. Kwon for insightful discussions on the climate data analysis and Kristian K. Kjeldsen for help with the digital elevation model image.

Figure captions

Fig. 1. Sermilik Fjord and Helheim Glacier with position of cores ER13 (660 m water depth), ER07 (525 m water depth) and ER11 (600 m water depth). The length of the fjord is c. 90 km and the width 5-12 km. The bathymetry is a compilation of data obtained during cruises conducted in recent years by Geological Survey of Denmark and Greenland, Woods Hole Oceanographic Institution, Swansea University and Nansen Environmental Remote Sensing Center (Supplementary Information). Background image is an oblique Landsat scene (L5231014_01419860911) draped over a digital elevation model.

Fig. 2. Sand (63-1000 μm) deposition rates (g m^{-2} yr^{-1}) in cores (1 sigma error bars a function of 1 sigma error of mass accumulation rates and sand content). a. ER11. b. ER07. c. ER13. d. Reconstructed calving record of Helheim Glacier (average of sand deposition rate in the three cores, Supplementary Information). ER13 chronology of composite record is adjusted towards a timescale two years older (within 1 sigma error bar) during the interval 1980-2000 to improve fit with glacier images (Fig. S3). Glacier margin positions (red) relative to 1993 position according to aerial and satellite images (Fig. S5 and Supplementary Information).

Fig. 3. Comparison between calving record and climate indices. a. Reconstructed calving record of Helheim Glacier. Grey line is unfiltered data. Increased calving events (HC1-HC10) are highlighted in red (intensity of calving indicated by different shading) and correspond to the residual variability. b. Annual mean SST for an area south of Iceland (20−30°W, 60−63°N) (Supplementary information). c. Storis Index[25]. d. Shelf Index (normalised AW temperature and Storis Index weighted 1:1). e. North Atlantic Oscillation (NAO) winter time Index[27]. f. T_{air} Summer (April-Sep) in Tasiilaq[26]. For b-f: black lines are 3 year running mean data and grey line is unfiltered data.

Table 1. Pearson correlation coefficient between calving and climate indices. Climate data were applied with a 3 yr running mean and all data were linearly detrended before computing r-values (bulk data). Multi-decadal variability highlighted by 25 year low-pass Fourier filtering and intra-decadal variability obtained as a residual after subtracting the low-pass filtered time series from the bulk data. For bulk data and residuals r-values >0.29 are statistically significant and for the low pass-filtered data r-values >0.74 are statistically significant at the 95% level. See also Supplementary Information.

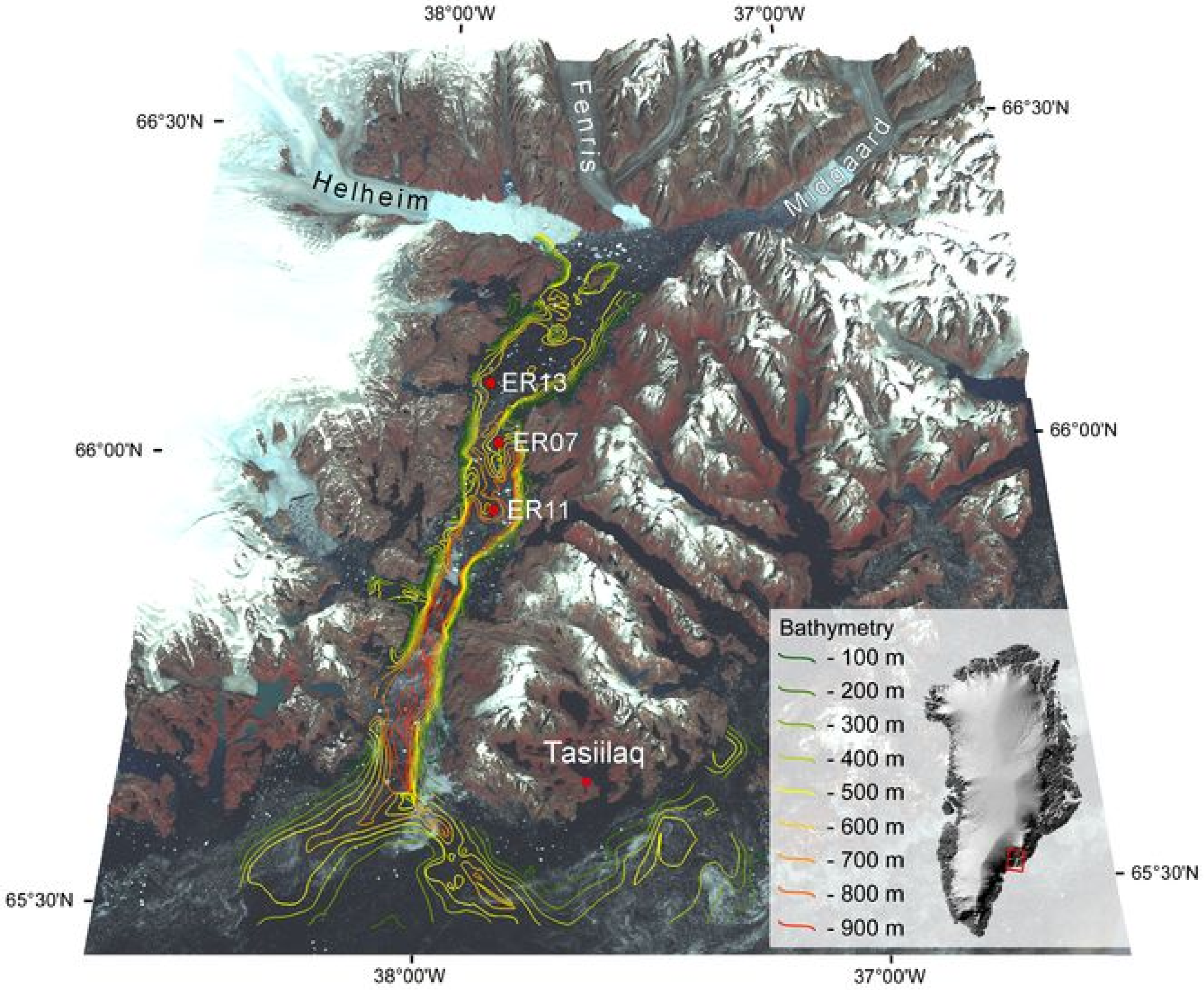
38°00'W
37°00'W
66°30'N
66°00'N
65°30'N
Helheim
Fenris
Midgaard
ER13
ER07
ER11
Tasiilaq
Bathymetry
- 100 m
- 200 m
- 300 m
- 400 m
- 500 m
- 600 m
- 700 m
- 800 m
- 900 m

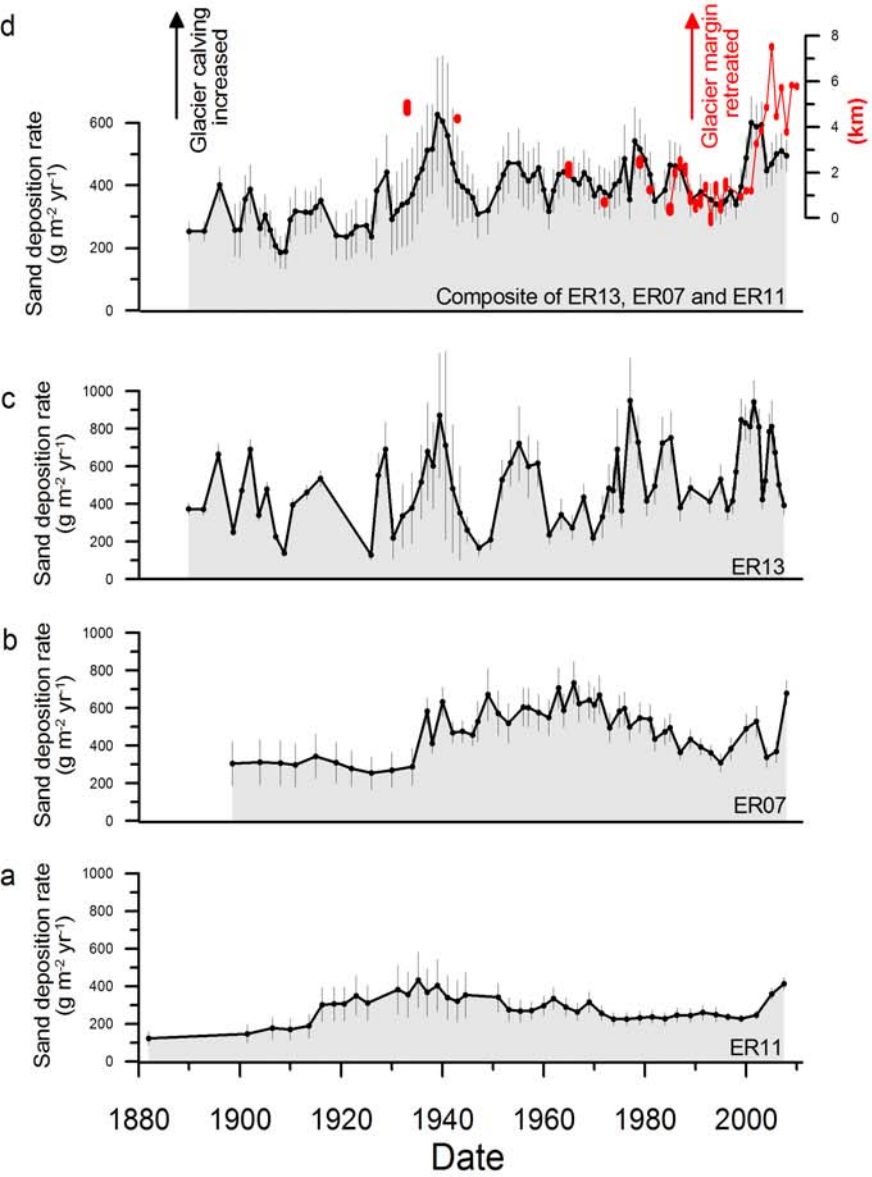
d
Glacier calving increased
Glacier margin retreated
(km)
Sand deposition rate (g m-2 yr-1)
Composite of ER13, ER07 and ER11
c
ER13
b
ER07
a
ER11
1880
1900
1920
1940
1960
1980
2000
Date

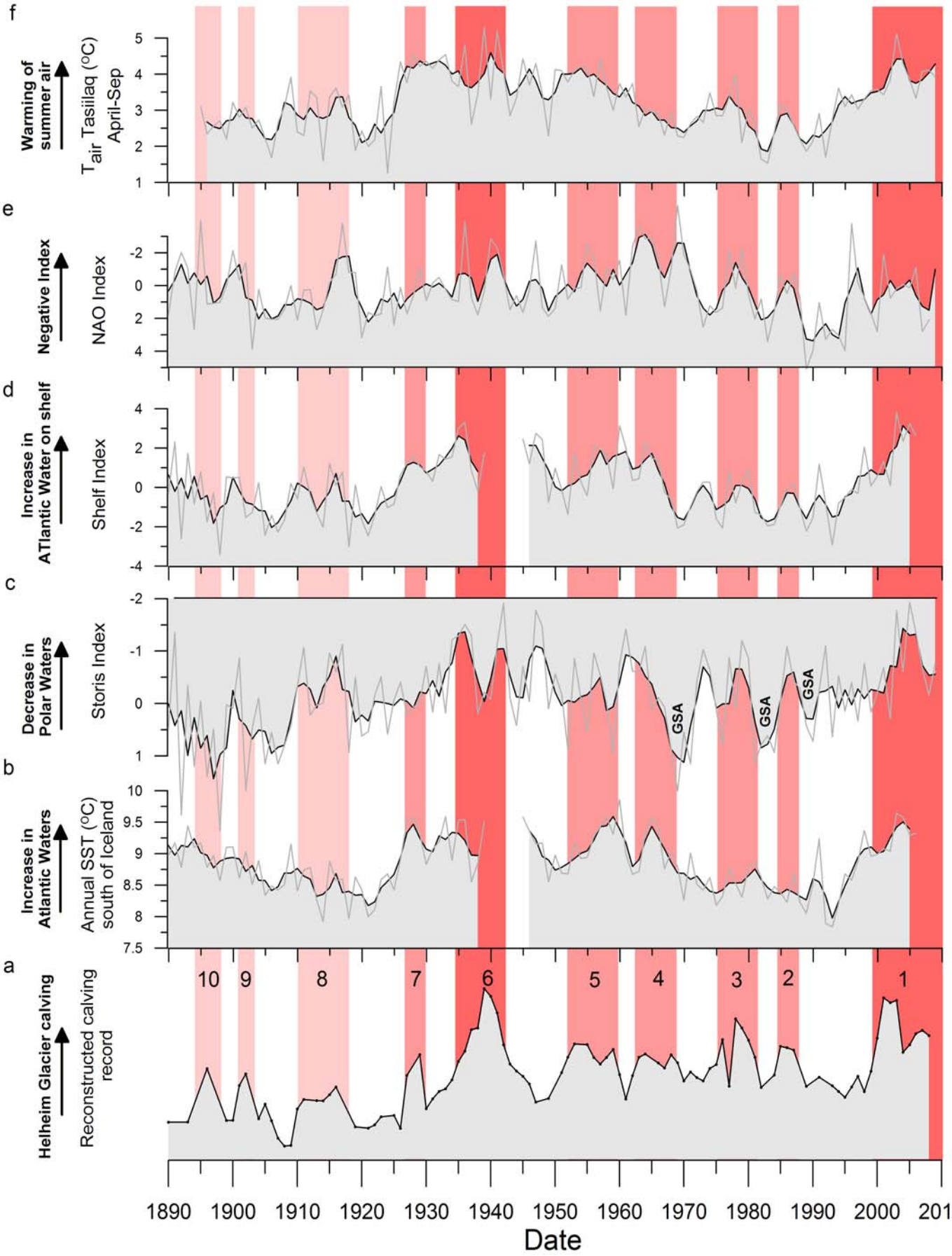
f
Warming of summer air
T_{air} Tasiilaq (°C) April-Sep
5
4
3
2
1
e
Negative Index
NAO Index
-2
0
2
4
d
Increase in ATlantic Water on shelf
Shelf Index
4
2
0
-2
-4
c
Decrease in Polar Waters
Storis Index
-2
-1
0
1
GSA
GSA
GSA
b
Increase in Atlantic Waters
Annual SST (°C) south of Iceland
10
9.5
9
8.5
8
7.5
a
Helheim Glacier calving
Reconstructed calving record
10
9
8
7
6
5
4
3
2
1
1890
1900
1910
1920
1930
1940
1950
1960
1970
1980
1990
2000
2010
Date

r-value with calving	T_{air} Summer	NAO Index	Storis Index	Atl. Water T_{annual}*	Shelf Index*
Bulk data (r≥0.29)	0.45	-0.45	-0.36	0.38	0.41
Multi-decadal variability (r≥0.74/0.75*)	0.73	-0.53	-0.61	0.72	0.69
Intra-decadal variability (r≥0.29)	0.24	-0.42	-0.18	0.27	0.29

Table 1